ORIGINAL ARTICLE

SRSF1 is essential for primary follicle development by regulating granulosa cell survival via mRNA alternative splicing

Xiaohong Yao[1] · Chaofan Wang[1] · Weiran Yu[1] · Longjie Sun[1] · Zheng Lv[1] · Xiaomei Xie[1] · Shuang Tian[1] · Lu Yan[1] · Hua Zhang[1] · Jiali Liu[1]

Abstract

Granulosa cell abnormalities are characteristics of premature ovarian insufficiency (POI). Abnormal expression of serine/arginine-rich splicing factor 1 (SRSF1) can cause various diseases, but the role of SRSF1 in mouse granulosa cells remains largely unclear. In this study, we found that SRSF1 was expressed in the nuclei of both mouse oocytes and granulosa cells. The specific knockout of *Srsf1* in granulosa cells led to follicular development inhibition, decreased granulosa cell proliferation, and increased apoptosis. Gene Ontology (GO) analysis of RNA-seq results revealed abnormal expression of genes involved in DNA repair, cell killing and other signalling pathways. Alternative splicing (AS) analysis showed that SRSF1 affected DNA damage in granulosa cells by regulating genes related to DNA repair. In summary, SRSF1 in granulosa cells controls follicular development by regulating AS of genes associated with DNA repair, thereby affecting female reproduction.

Keywords SRSF1 · Granulosa cell · Alternative splicing · DNA damage

Introduction

The main function of the ovary is to produce germ cells (oocytes) [1]. The ovaries comprise oocytes, granulosa cells, and theca cells, among which oocytes provide genetic material. Oocytes and somatic cells exchange many regulatory signals that control oocyte metabolism, cytoskeletal remodelling, cell cycle progression, and fertilization, all of which are key events that initiate and maintain early embryogenesis [2–4]. Problems in any of the cell types in the ovary can lead to infertility in females.

POI affects female fertility. The histological characteristics of POI indicate that most follicles are histologically abnormal, and the follicles are atretic, characterized by partial to complete absence of granulosa cells [5, 6]. Ovarian granulosa cells in patients with POI exhibit significant changes in their proteomes, and a total of 2688 proteins have been identified, 70 of which are significantly differentially expressed [7]. Abnormal AS is one of the causes of POI. TP63 (human)/Trp63 (mouse) produces various AS isomer products at the C-terminus associated with female infertility, including POI [8]. A missense mutation in the HFM1 gene (c.3470G > A) alters the splicing of its mRNA in the ovary and may be one of the causes of POI [9].

mRNA splicing requires a set of fundamental factors called SR proteins. SRSF1 is the classic member of the SR protein family, and it is involved in the maturation of the spliceosome [10–12]. SRSF1 plays an integral role in maintaining cell homeostasis by regulating many complex biological pathways [13]. SRSF1 deficiency is associated with a variety of diseases; for example, SRSF1 regulates AS in breast cancer [14], promotes mammary epithelial cell transformation [15], regulates gene expression in the immune system [16], regulates T-cell homeostasis and function [17], promotes the proliferation, migration, invasion of hepatocellular carcinoma [18] and regulates primordial follicle formation and number determination during meiotic prophase I [19]. A previous study showed that SRSF1 inhibits porcine granulosa cell apoptosis and follicular atresia through a circSLC41A1-miR-9820-5p-SRSF1 regulatory axis [20]. However, the role of SRSF1 in granulosa cell development in vivo has not been described.

Xiaohong Yao, Chaofan Wang have contributed equally.

✉ Jiali Liu
liujiali@cau.edu.cn

1 State Key Laboratory of Animal Biotech Breeding, College of Biological Sciences, China Agricultural University, Beijing 100193, China

To explore the function of SRSF1 in granulosa cells, we used *Foxl2-CreER^{T2}* mice to knock out *Srsf1* specifically. The specific deletion of *Srsf1* in granulosa cells resulted in follicular development inhibition, decreased granulosa cell proliferation, and increased apoptosis. RNA-seq results showed that SRSF1 directly regulated the AS of genes related to DNA repair.

Materials and methods

Mice

C57BL/6 mice were obtained from Beijing Vital River Laboratory Animal Technology Co., Ltd. *Srsf1^{F/F}* mice and *Foxl2-CreER^{T2}* mice were generated as previously reported [21, 22]. *Srsf1^{F/F}* mice were generated in the laboratory of Prof. Xiangdong Fu (University of California, San Diego, USA) and kindly provided by Prof. Yuanchao Xue (Institute of Biophysics, Chinese Academy of Sciences, Beijing, China). To knockout *Srsf1* in mouse ovarian granulosa cells as early as possible, the mice were injected with 20 mg/kg tamoxifen (T5648; Sigma, St. Louis, MO, USA) at 1 day postpartum (dpp), 3 dpp, and 5 dpp to activate Cre recombinase. All the mice were housed in the pathogen-free Animal Care Facility of China Agricultural University under a 12-h light/12-h dark cycle at an ambient temperature of 21 ± 2 °C, and they were given free access to food and water.

Identification of mouse genotypes

DNA was extracted from mouse tails using the HotSHOT method, and PCR was used for genotyping. The PCR primers used are listed in Supplementary Table 1. The PCR conditions were as follows: 95 °C for 5 min; 36 cycles of 95 °C for 30 s, 55 °C for 30 s, and 72 °C for 40 s; 72 °C for 5 min; and holding at 4 °C. The primers produced PCR products of 346 bp for the wild-type *Srsf1* allele and 386 bp for the floxed allele.

Histological analysis of ovary and follicle counts

Ovaries were prepared for histological analysis by immediately placing them in cold 4% paraformaldehyde for fixation. Fixation was performed overnight at 4 °C, and ovaries were transferred to 70% ethanol, dehydrated, and embedded in paraffin. Tissues were sectioned at a thickness of 5 μm. Tissue sections were stained with hematoxylin.

The ovarian sections were analyzed with a slide scanner (VENTANA DP 200, Roche, Switzerland), and the follicles were counted in all sections with clear oocyte nuclei. Every five ovarian sections were analysed. There are five types of follicles: primordial follicles, primary follicles, secondary follicles, antral follicles, and atretic follicles, according to the morphology and number of granulosa cell layers [23].

Immunofluorescence (IF) staining

Ovarian sections were dewaxed and then microwaved in 0.01 M sodium citrate buffer (pH = 6.0) for antigen retrieval. The prepared sections were blocked with 10% normal goat serum (SP-9000; Zhongshan Golden Bridge Biotechnology, Beijing, China) for 1 h at room temperature (RT) and then incubated with the indicated primary antibodies (Table S2). After being washed three times with PBS, the samples were incubated with the indicated secondary antibodies (Table S2) at a 1:400 dilution for 2 h at RT and with 4′,6-diamidino-2-phenylindole (DAPI) (10236276001; Roche Applied Science, Basel, Switzerland) at RT for 10 min. The slides were washed three times in PBS and mounted with anti-fade mounting medium (P0128S; Beyotime Biotechnology, Shanghai, China). Finally, a Nikon A1 laser scanning confocal microscope (A1, Nikon, Japan) was used for image acquisition.

TUNEL

TUNEL assays were performed on 4% paraformaldehyde-fixed paraffin-embedded sections using the One Step TUNEL Apoptosis Assay Kit (C1088; Beyotime Biotechnology, Shanghai, China) according to the manufacturer's instructions.

Cell proliferation assay

Mice were injected with 100 mg/kg 5-bromo-2′-deoxyuridine (BrdU) (B5002, Sigma, St. Louis, MO, USA) in a physiological saline solution by intraperitoneal injection. After 2 h, mouse ovaries were fixed and embedded in paraffin. Then, tissue sectioning, antigen retrieval, BrdU staining, and image acquisition were conducted as described in the IF methods.

Western blot

The ovaries were lysed in RIPA buffer (P0013B; Beyotime Biotechnology, Shanghai, China) and homogenized with a grinding rod. The protein extracts were subjected to electrophoresis on 12% sodium dodecyl sulfate–polyacrylamide gels and transferred to polyvinylidene difluoride membranes (IPVH00010; Millipore, USA). The membranes were blocked with 5% nonfat milk (P0216-300 g; Beyotime Biotechnology, Shanghai, China) prepared in Tris-buffer saline plus 0.1% Tween-20 (TBST) at RT for 1 h and then incubated with primary antibodies overnight at 4 °C. Then,

the membranes were incubated with secondary antibodies (Table S2) for 2 h. After washing with TBST three times, the membranes were visualized with BeyoECL Plus (P0018S; Beyotime Biotechnology, Shanghai, China) with the ECL system (5200, Tanon, China).

Quantitative real-time PCR (qPCR) and reverse transcription PCR (RT−PCR)

Total RNA was extracted by TRIzol Reagent (9109; TaKaRa, Dalian, China). One microgram of total RNA was used to synthesize first-strand cDNA (M170A; Promega, USA).

qPCR analysis was performed with Hieff UNICON® qPCR SYBR Green Master Mix (11198ES03; YEASEN, Shanghai, China). cDNA was diluted and used as the template for the real-time SYBR Green assay. *Gapdh* was used as the endogenous control. All gene expression was quantified relative to *Gapdh* expression (Table S3).

RT−PCR analysis was performed with cDNA using $2 \times$ Taq Master Mix (Dye Plus) for common PCR, and mature mRNA sequences were used to design primers for RT−PCR (Table S4).

RNA immunoprecipitation (RIP)

Ovaries were lysed with cell lysis buffer (P0013, Beyotime Biotechnology, Shanghai, China). First, RNase inhibitor (1:20, R0102, Beyotime Biotechnology, Shanghai, China) was added. Two micrograms of IgG (A7016, Beyotime Biotechnology, Shanghai, China) and SRSF1 antibody (12929–2-AP, Proteintech, Chicago, USA) were bound to BeyoMag™ Protein A (P2102-1 ml, Beyotime Biotechnology, Shanghai, China). 10% of the ovary lysate supernatants were used as the input, and the remaining volume was incubated with BeyoMag™ Protein A overnight at 4 °C. Bound RNA was extracted using a Direct-zol RNA Microprep Kit (R2060, Zymo Research, Los Angeles, USA) and analysed by RT−qPCR analysis.

RNA-seq

We called primordial follicular granulosa cells as pfGCs. For the convenience of description, *Srsf1*$^{F/F}$ mice are called PfGC- *Srsf1*$^{+/+}$, *Srsf1*$^{F/F}$; *Foxl2-CreER*^{T2} mice are called PfGC- *Srsf1*$^{-/-}$. Ovarian samples were collected from PfGC- *Srsf1*$^{+/+}$ and PfGC- *Srsf1*$^{-/-}$ mice at 8 dpp and sent to Novogene for RNA-seq analysis. Total RNA was isolated, and the quality of RNA samples was controlled by an Agilent 2100 bioanalyzer (2100, Agilent, USA). mRNA was randomly divided into fragments with fragmentation buffer, and the database was built in standard NEB mode. Sequencing was performed using an Illumina NovaSeq 6000 (Illumina,

USA). Significant gene expression differences were analyzed, and GO enrichment analysis was conducted using clusterProfiler (version 3.8.1) software. AS was analyzed using rMATS (version 4.1.0) software.

Cell culture and cell transfection

The KK1 cell line was cultured in DMEM/F12 (C11330500BT, Gibco, USA) containing 10% fetal bovine serum (S500, Newzerum, Ltd., Christchurch, New Zealand) and 1% penicillin and streptomycin at 37 ℃ in a 5% CO_2 incubator. The sequences were as follows: NC, sense (5´-3´): UUCUCCGAACGUGUCACGUTT;

antisense (5´-3´): ACGUGACACGUUCGGAGAATT;
siRNA-361, sense (5´–3´): GGGUUUGGAGGAUUU GGAATT; antisense (5´–3´): UUCCAAAUCCUCCAAACC CTT; siRNA-1204, sense (5´–3´): GCAGGUGUUGAUCCU AUUATT; antisense (5´–3´): UAAUAGGAUCAACACCUG CTT; siRNA-541, sense (5´–3´): GGACUUGGAUUUGGA GGAUTT; antisense (5´–3´): AUCCUCCAAAUCCAAGUC CTT; siRNA-1002, sense (5´–3´): GGAUGAUCAGACGGA AGUUTT; antisense (5´–3´): AACUUCCGUCUGAUC AUCCTT; siRNA was transfected into the KK1 cell line using Lipo8000™ (C0533; Beyotime Biotechnology, Shanghai, China) according to the manufacturer' s instructions.

Statistical analysis

All the statistical analyses were performed with GraphPad Prism software (version 7.0) using Student' s *t*-test. The data are presented as the means ± SEMs at least three independent experiments. $P < 0.05$ was considered statistically significant. *$P < 0.05$, **$P < 0.01$, ***$P < 0.001$, ****$P < 0.0001$. Mouse genome data (GRCm39) were used as the reference.

Results

## Expression pattern of SRSF1 in mouse ovaries

To explore the function of SRSF1 in mouse ovarian granulosa cells, we first characterized the SRSF1 expression pattern during follicle development. qPCR analyses of ovaries on different days showed that *Srsf1* mRNA expression increased from 1 dpp to 21 dpp (Fig. 1A). Western blot was used to measure the protein expression level of SRSF1. The results were consistent with the qPCR results (Fig. 1B). To further determine the localization of SRSF1 in mouse ovaries, we conducted IF, and SRSF1 was highly expressed in the nuclei of oocytes and granulosa cells (Fig. 1C). These data suggest that SRSF1 in granulosa cells may play essential roles in ovary development.

Fig. 1 Expression pattern of SRSF1 during follicular development. **A** Relative *Srsf1* mRNA expression levels in ovaries on different days. Student' s *t*-test was used for statistical analysis.The results are presented as the means±SEMs. Three independent experiments were performed for each data. **B** The SRSF1 protein levels were measured by Western blot on different days. Student' s *t*-test was used for statistical analysis. The results are presented as the means±SEMs. *n*=4. **C** The localization of SRSF1 in 1 dpp, 7 dpp, 14 dpp, and 21 dpp ovaries was determined by IF. Scale bars, 100 μm
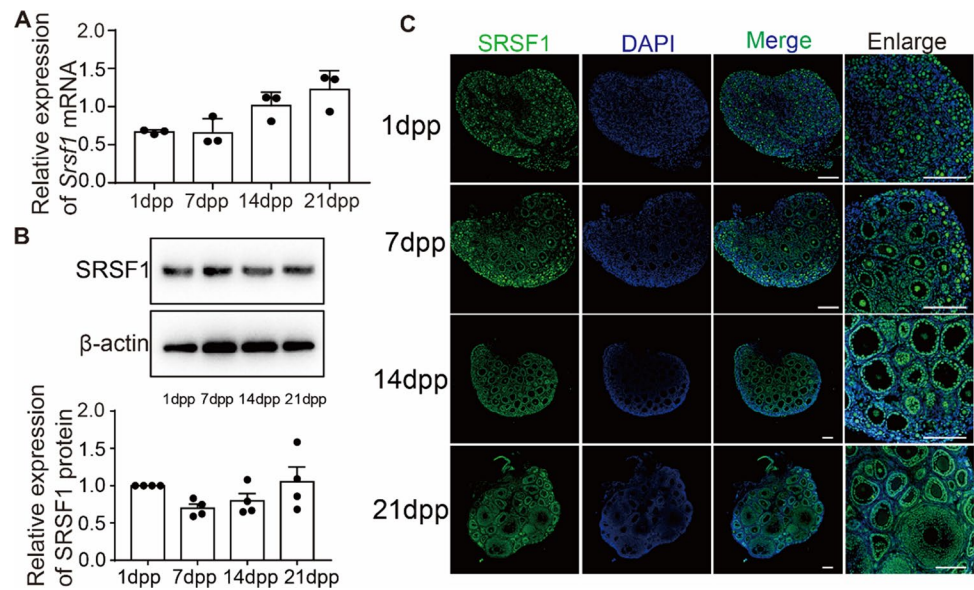
Fig. 2 SRSF1 was successfully knocked out in granulosa cells at 7 dpp. **A** Injection of tamoxifen to induced knock out exon. **B** WT; *Srsf1^{F/+}*; *Foxl2-CreER^{T2}*, and *Srsf1^{F/F}*; *Foxl2-CreER^{T2}* genotype determination. **C** Localization of SRSF1 in PfGC-*Srsf1^{+/+}* and PfGC-*Srsf1^{-/-}* ovary. The area indicated by the dashed white circle represents granulosa cells. Scale bars, 50 μm
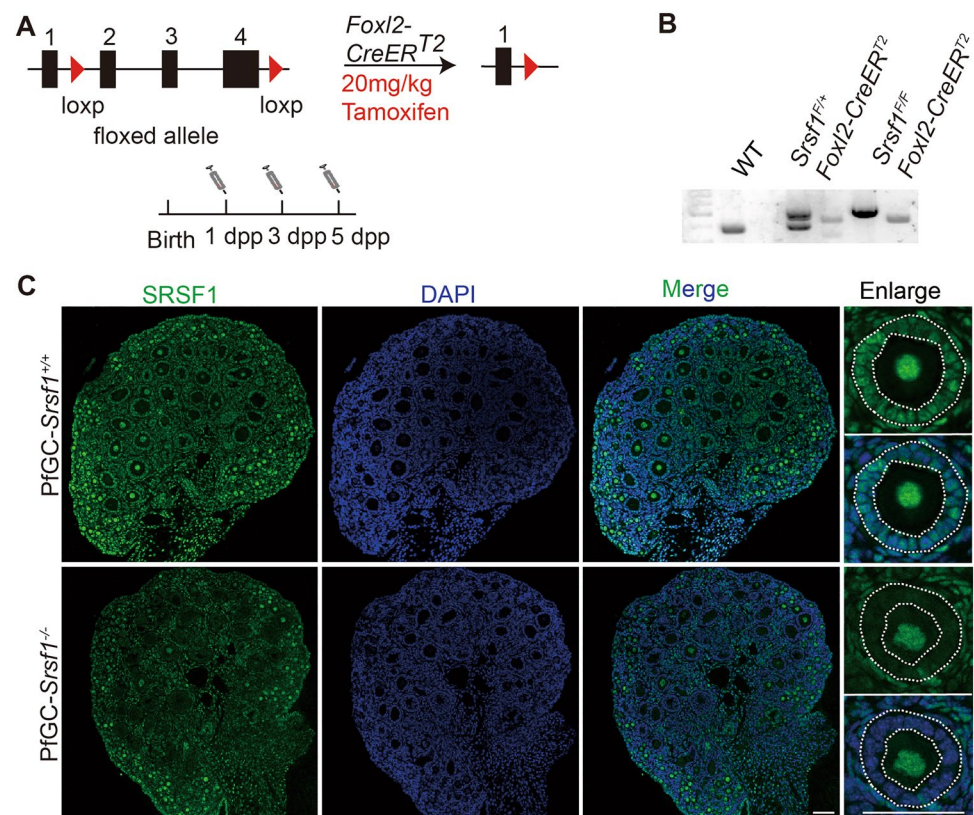
SRSF1 was absent in granulosa cells of primary follicles in *Srsf1^{-/-}* ovaries

To study the role of SRSF1 in granulosa cells, mice with the *Srsf1* conditional floxed allele (*Srsf1^{Fl/Fl}*), in which exons 2, 3, and 4 of *Srsf1* were flanked by two *loxP* sites, were crossed with *Foxl2-CreER^{T2}* mice (Fig. 2A, S1A). To activate the Cre enzyme, mice were injected with 20 mg/kg of tamoxifen every another day, starting on 1 dpp and ending on 5 dpp (Fig. 2A). Mouse genotypes were determined by PCR (Fig. 2B). IF showed a specific loss of SRSF1 in primary follicular granulosa cells at 7

dpp (Fig. 2C). However, SRSF1 was still present in the pfGCs (Fig. S1B), which may be due to the accumulation of undegraded SRSF1 protein in PfGCs.

Knockout of *Srsf1* in ovarian granulosa cells resulted in follicular development arrest

To further identify the function of SRSF1 in granulosa cells, we used haematoxylin staining to distinguish the differences in ovarian histology on different days in PfGC-*Srsf1*$^{+/+}$ and PfGC-*Srsf1*$^{-/-}$. The histological analyses at 7 dpp revealed that PfGC-*Srsf1*$^{+/+}$ and PfGC-*Srsf1*$^{-/-}$ contained primordial follicles and primary follicles (Fig. 3A-a–d). We counted whole ovarian follicles and found that PfGC-*Srsf1*$^{+/+}$ and PfGC-*Srsf1*$^{-/-}$ did not differ significantly in the numbers of primordial follicles and primary follicles, while the number of secondary follicles was reduced in PfGC-*Srsf1*$^{-/-}$ compared with PfGC-*Srsf1*$^{+/+}$ (Fig. 3B). These results suggest that the loss of *Srsf1* in granulosa cells leads to the inhibition of follicular development. At 14 dpp, there was a difference in ovarian sizes between PfGC-*Srsf1*$^{+/+}$ and PfGC-*Srsf1*$^{-/-}$ (Fig. 3A-e, g). When the total number of follicles remained unchanged, more follicles in PfGC-*Srsf1*$^{+/+}$

developed into secondary follicles, but few primary follicles developed into secondary follicles in PfGC-*Srsf1*$^{-/-}$, and the number of atretic follicles in PfGC-*Srsf1*$^{-/-}$ significantly increased (Fig. 3B). At 21 dpp, the difference in ovarian morphology was more pronounced between PfGC-*Srsf1*$^{+/+}$ and PfGC-*Srsf1*$^{-/-}$ (Fig. 3A-i, k). The follicle counts at 21 dpp showed the same trend as those at 14 dpp. There was no significant difference in the total number of follicles between PfGC-*Srsf1*$^{+/+}$ and PfGC-*Srsf1*$^{-/-}$, but compared with the PfGC-*Srsf1*$^{+/+}$ group, the PfGC-*Srsf1*$^{-/-}$ group had fewer secondary follicles, and antral follicles, while the number of atretic follicles was increased (Fig. 3B). These data revealed that specific knockout of *Srsf1* in ovarian granulosa cells could lead to follicular development arrest, and many follicles of the PfGC-*Srsf1*$^{-/-}$ group were blocked in the primary follicle stage.

Loss of SRSF1 led to abnormal proliferation and apoptosis in granulosa cells

The absence of secondary follicles in mouse PfGC-*Srsf1*$^{-/-}$ suggests that granulosa cell proliferation and apoptosis may be abnormal. To test our hypothesis, we examined

Fig. 3 Loss of SRSF1 in granulosa cells led to follicular development arrest. **A** Follicular morphology of PfGC-*Srsf1*$^{+/+}$ and PfGC-*Srsf1*$^{-/-}$ at 7 dpp, 14 dpp and 21 dpp ovary. The red boxes represent atretic follicles in figure A-h,l. Black scale bars, 100 μm; white scale bars, 1 mm. **B** The numbers of ovarian follicles of PfGC-*Srsf1*$^{+/+}$ and PfGC-*Srsf1*$^{-/-}$ at 7 dpp, 14 dpp, and 21 dpp were counted. PrF, primordial follicles; PF, primary follicles; SF, secondary follicles; AF, antral follicles; ATF, atretic follicles. Student's *t*-test was used for statistical analysis. The data are presented as the means ± SEMs. $n = 3$. *$P < 0.05$, **$P < 0.01$, ***$P < 0.001$, ****$P < 0.0001$
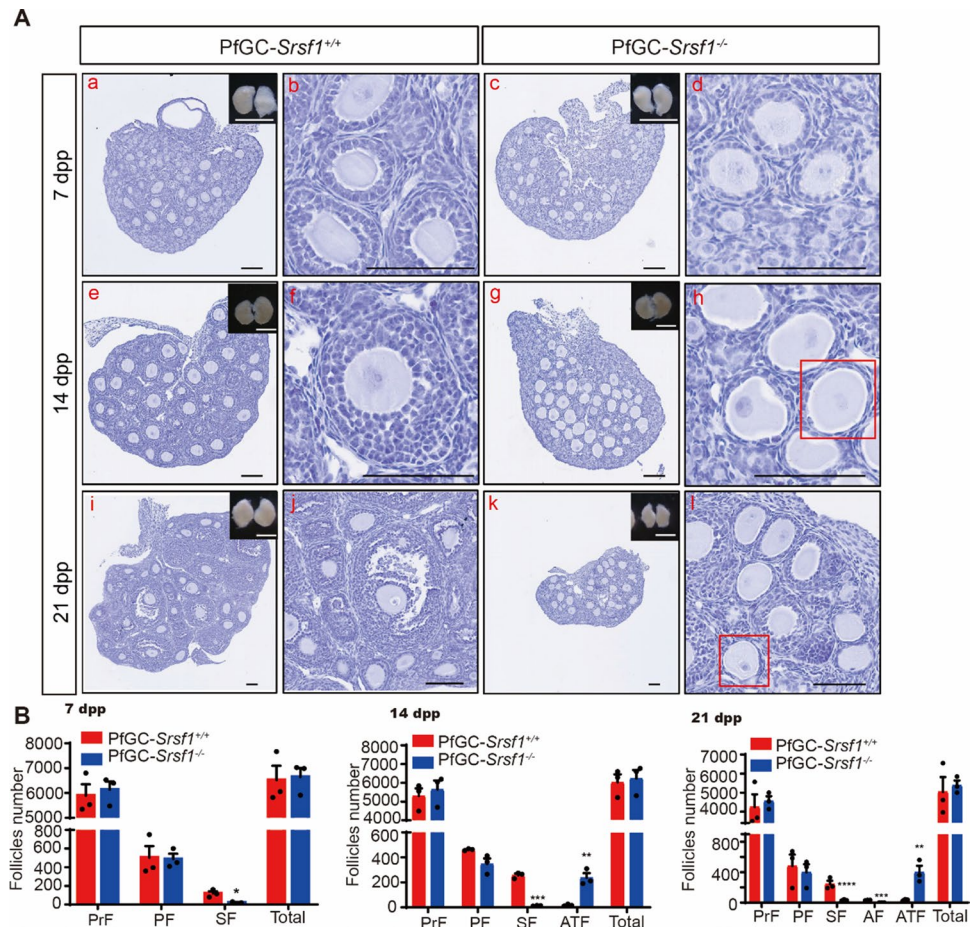
Fig. 4 Loss of SRSF1 affected granulosa cell proliferation and apoptosis. **A** BrdU signal in 7 dpp ovaries were detected by IF. Scale bars, 50 μm. **B** The percentage of BrdU$^+$ cells among granulosa cells. Student' s t-test was used for statistical analysis. The data are presented as the means ± SEMs. $n = 3$. **$P < 0.01$. **C** Images of PfGC- $Srsf1^{+/+}$ and PfGC- $Srsf1^{-/-}$ ovaries were obtained after TUNEL staining at 7 dpp, 10 dpp and 14 dpp. Scale bars, 100 μm. **D** The TUNEL-positive cell proportion was determined at different times. Student' s t-test was used for statistical analysis. The data are presented as the means ± SEMs. $n = 3$. **$P < 0.01$
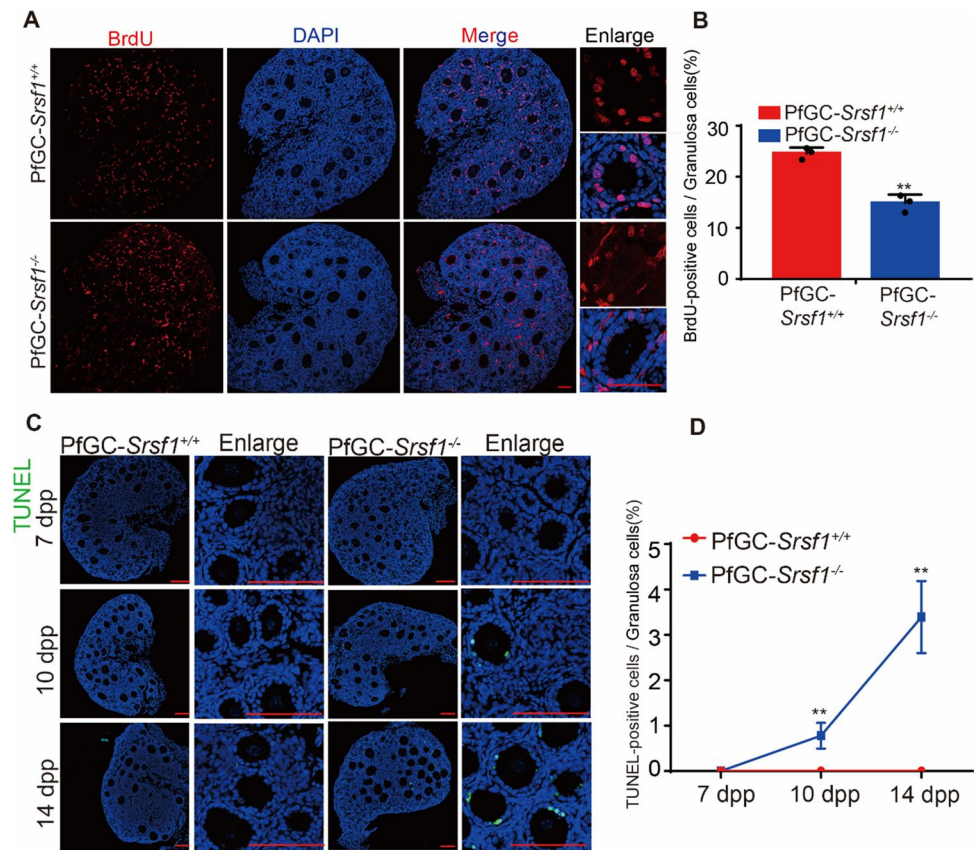

granulosa cell proliferation by BrdU incorporation at 7 dpp (Fig. 4A). Cell counting results showed that the BrdU immunoreactive (BrdU$^+$) cell ratio in PfGC-$Srsf1^{-/-}$ was significantly lower than that in PfGC-$Srsf1^{+/+}$ (Fig. 4B), indicating that the proliferation rate of PfGC-$Srsf1^{-/-}$ was decreased. Furthermore, we examined the apoptosis of granulosa cells. The TUNEL results showed no positive cells in PfGC-$Srsf1^{+/+}$ at 7 dpp, 10 dpp, and 14 dpp. However, the apoptosis of PfGC-$Srsf1^{-/-}$ occurred at 10 dpp and increased at 14 dpp (Fig. 4C, D), and granulosa cell apoptosis occurs in follicles that are transformed from primary follicles to secondary follicles. These results suggest that knockout $Srsf1$ in granulosa cell can slow granulosa cell proliferation and increase apoptosis, ultimately leading to follicular atresia.

SRSF1 deficiency in granulosa cells resulted in abnormal ovarian transcriptome

To investigate changes in gene expression after $Srsf1$ deletion in granulosa cells, we performed RNA-seq sequencing on ovaries from PfGC- $Srsf1^{+/+}$ and PfGC-$Srsf1^{-/-}$ mice at 8 dpp. The correlation coefficients within and between the groups were calculated according to the FPKM values of all the genes in each sample. The squared Pearson correlation coefficients (R^2) of the gene expression levels between samples were more significant than 0.92, indicating that the experiment was reliable and that the sample selection was reasonable (Fig. S2A). We found that 1543 genes were differentially expressed, with 881 upregulated and 662 downregulated genes in PfGC-$Srsf1^{-/-}$ ovaries (Fig. 5A). Cluster analysis was performed on the differential gene sets, and genes with similar expression patterns were grouped. The differentially expressed genes in the control and knockout groups are presented as a clustered heatmap (Fig. 5B). We then performed GO analysis to identify the enriched biological processes for each group of differentially expressed genes (DEGs). The upregulated genes in PfGC-$Srsf1^{-/-}$ were significantly involved in autophagy, reproductive system development, regulation of apoptotic signalling pathway, signal transduction by p53 class mediator, ERK1 and ERK2 cascade, and cell killing (Fig. 5C). The downregulated genes in PfGC-$Srsf1^{-/-}$ were significantly involved in the regulation of DNA repair, cAMP biosynthetic process and so on (Fig. 5D). Cluster analysis of the upregulated and downregulated signalling pathways of cell killing, regulation of the apoptotic pathway, signal transduction by p53 class mediators and regulation of DNA repair indicated that the knockout of SRSF1 in ovarian granulosa cells affected multiple biological processes that lead to cell apoptosis (Fig. S2B).

Fig. 5 SRSF1 deficiency in granulosa cells altered gene expression patterns. **A** Volcano plot showing the distribution of differentially expressed genes identified by RNA-seq. ($p$value < = 0.05, |log2Fold-Change|> = 0). **B** Heatmap of the DEGs between PfGC-*Srsf1*$^{+/+}$ and PfGC-*Srsf1*$^{-/-}$ at 8 dpp. **C** GO analysis of upregulated genes in PfGC-*Srsf1*$^{-/-}$. The overrepresented terms, gene counts, and qValue are shown. **D** GO analysis of downregulated genes in PfGC-*Srsf1*$^{-/-}$. The overrepresented terms, gene counts, and qValue are shown. **E** The mRNA expression of 8 dpp ovaries. Student's t-test was used for statistical analysis. The data are presented as the means ± SEMs. $n = 3$. *$P < 0.05$, **$P < 0.01$, ***$P < 0.001$, ****$P < 0.0001$
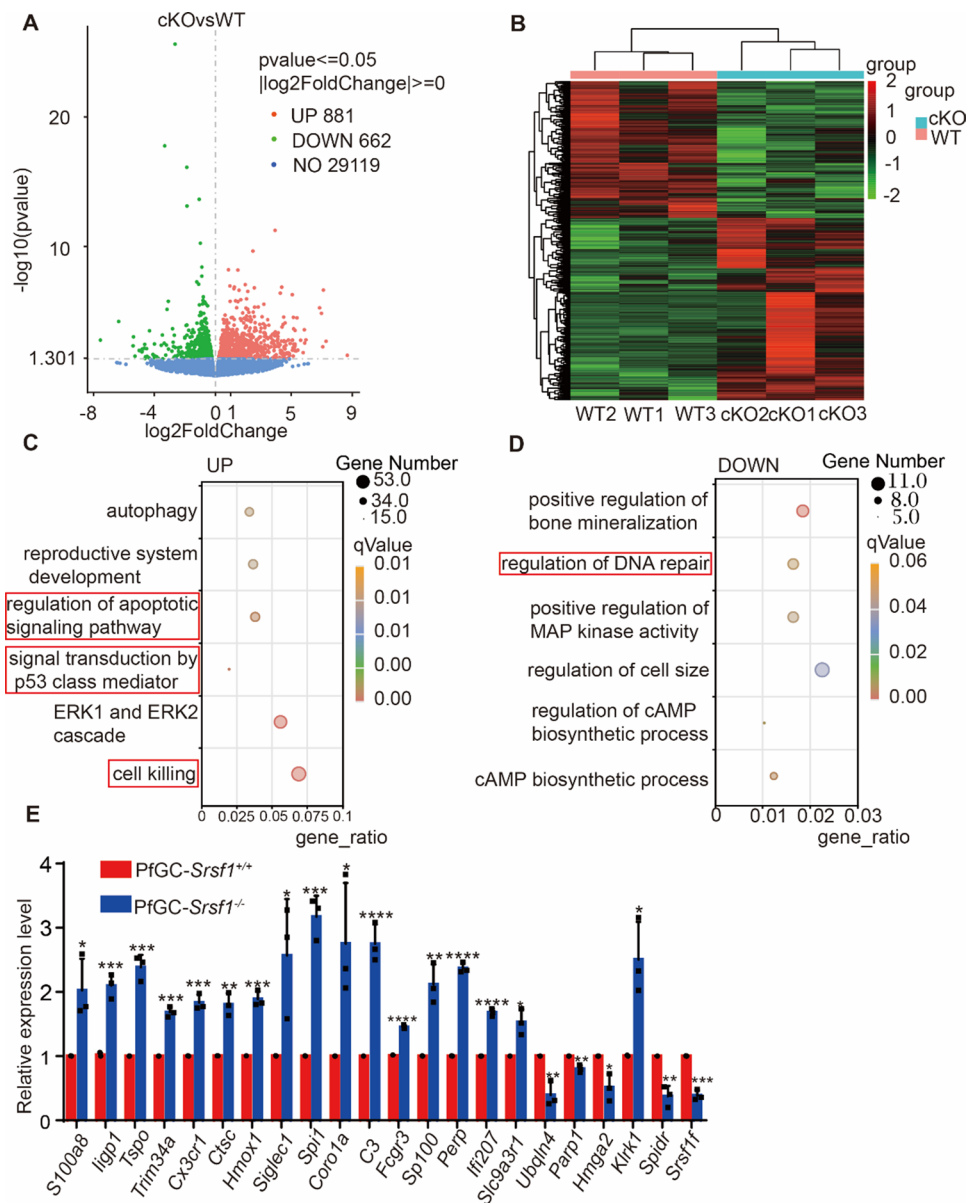

Moreover, qPCR was used to verify the expression of related genes. The qPCR results were consistent with the RNA-seq results (Fig. 5E).

SRSF1 participated in AS affecting DNA repair

AS is essential for regulating gene expression and generating proteome diversity. Data analysis on cKO vs. WT showed that 249 genes underwent AS, of which 29 splicing events were classified as alternative 3′ splice sites (A3SS), 34 splicing events were classified as alternative 5′ splice sites (A5SS), 142 splicing events were classified as skipped exons (SE), 28 splicing events were classified as retained introns (RI), and 16 splicing events were classified as mutually exclusive exons (MXE) (Fig. 6A). SE accounted for the highest proportion (Fig. 6B). The GO enrichment analysis of AS revealed that lysosome organization, regulation of apoptotic signalling pathway, DNA repair, negative regulation of translation, mitotic spindle organization, negative regulation of growth, and single-stranded RNA binding-related genes were associated alterations in AS form (Fig. 6C). We used Integrative Genomics Viewer (IGV, version 2.10.2) software to visualize AS, and RT−PCR was used to analyze AS patterns (Fig. S3A). Therefore, we successfully validated the AS of four DNA repair-related genes. The results showed that *Chd1l* has an A5SS splicing form, and *Herc2, Usp3,* and *Nup54* have SE AS forms. Using RT−PCR verification, the results showed that SRSF1 regulates the AS of *Chd1l, Herc2, Usp3,* and *Nup54* pre-mRNA in the ovary, thus affecting DNA repair (Fig. 6D). Western blot results

Fig. 6 SRSF1 participation in AS affected DNA repair. **A** Different types of AS are caused by SRSF1 deficiency in granulosa cells. **B** The proportions of different types of AS are shown in pie charts. **C** GO enrichment analysis of AS events. **D** Splicing pattern and RT-PCR validation of *Chd1l*, *Herc2*, *Usp3*, and *Nup54*. Integrative Genomics Viewer (IGV, version 2.10.2) was used to visualize and confirm AS events in RNA-seq data. **E** Western blot results revealed the NUP54 and USP3 protein levels in PfGC- *Srsf1*$^{+/+}$ and PfGC- *Srsf1*$^{-/-}$ ovaries. Student's *t*-test was used for statistical analysis. The data are presented as the means ± SEMs. *n* = 3. *P < 0.05. **F** The results of RIP enrichment. Student's *t*-test was used for statistical analysis. The data are presented as the means ± SEMs. *n* = 3. *P < 0.05, ***P < 0.001, ****P < 0.0001. **G** Images of PfGC- *Srsf1*$^{+/+}$ and PfGC- *Srsf1*$^{-/-}$ ovaries were obtained at 7 dpp, 10 dpp, and 14 dpp after staining for γ-H2AX. Scale bars, 100 μm. **H** The proportion of γ-H2AX-positive cells was counted at different times. Student's *t*-test was used for statistical analysis. *n* = 3. ***P < 0.001
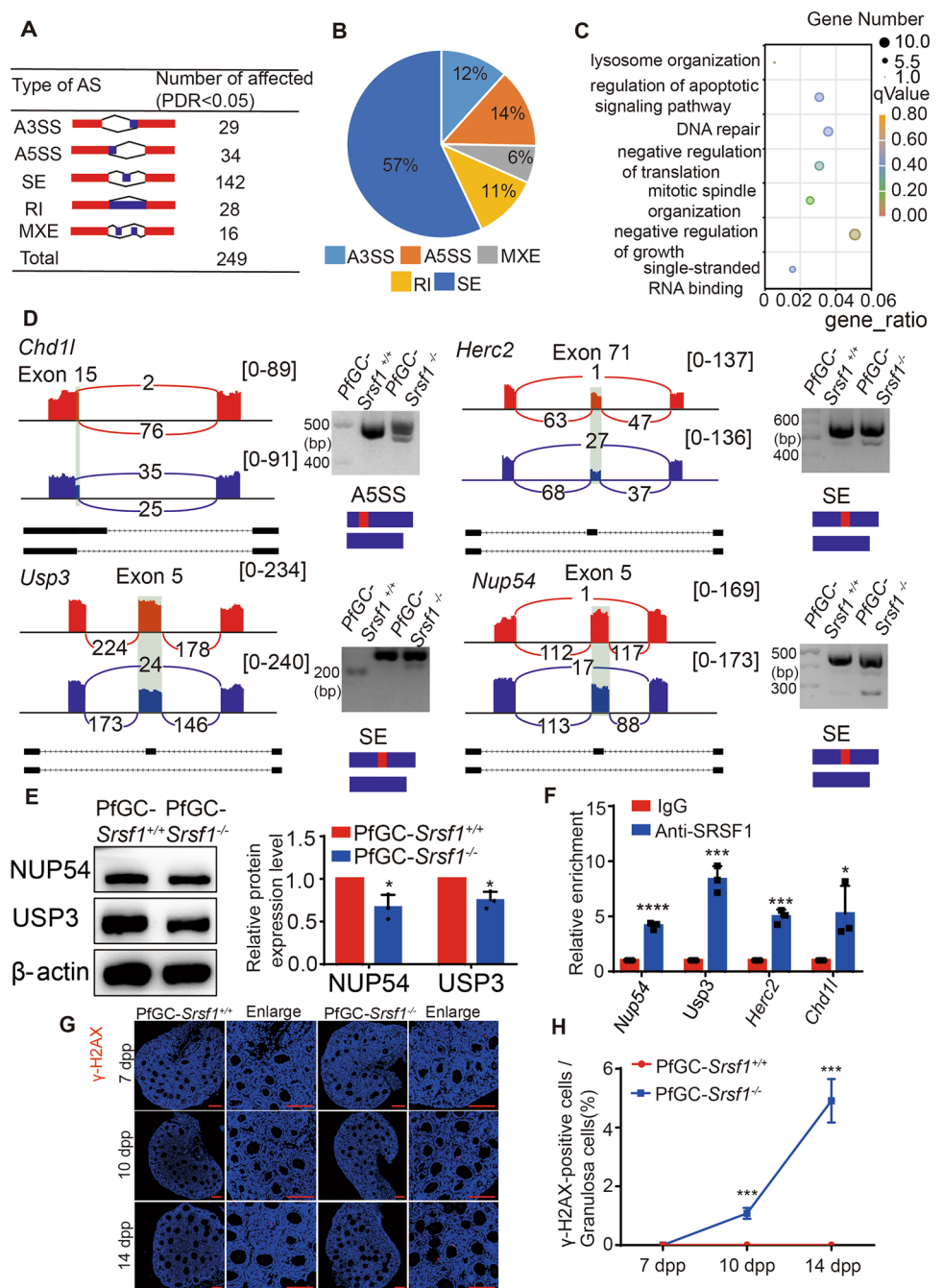

showed that NUP54 and USP3 protein levels were significantly decreased (Fig. 6E). In addition, the results revealed that PPT1 and NDUFS3 protein levels were reduced (Fig. S3B). RIP was used to verify whether SRSF1 directly binds to RNA, and the verification results showed that genes were significantly enriched in the anti-SRSF1 group, indicating that SRSF1 directly binds to pre-mRNA and participates in AS (Fig. 6F) (Fig. S3C). To further verify whether *Srsf1* deletion affects DNA repair in ovarian granulosa cells, granulosa cells were stained with γ-H2AX at 7 dpp, 10 dpp, and 14 dpp. The results showed no positive cells among

PfGC-*Srsf1*$^{+/+}$ at 7 dpp, 10 dpp, and 14 dpp, whereas DNA damage increased in granulosa cells from 10 to 14 dpp in the PfGC-*Srsf1*$^{-/-}$ group (Fig. 6G, H), suggesting that *Srsf1* deletion leads to irreparable DNA damage through abnormal AS.

To detect whether deletion of *Nup54* in KK1 cell lines leads to DNA damage, we successfully knocked down *Nup54* in KK1 cell lines using siRNA, siRNA-1204 has the highest interference efficiency (Fig. S4A). Immunofluorescence results showed that the percent of the γ-H2AX positive cell in knockdown group was large than

Fig. 7 Schematic diagram of the mechanism by which SRSF1 regulates granulosa cell survival
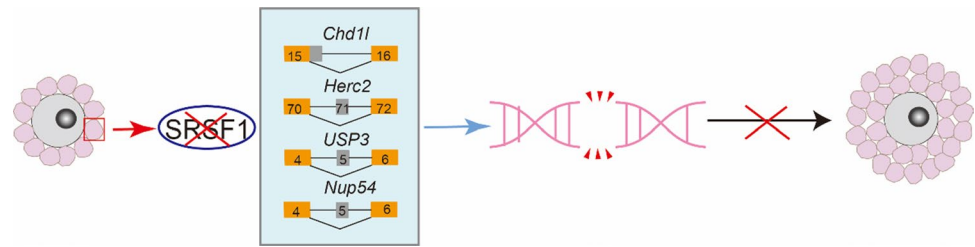
in control group, indicating that DNA damage occurred in KK1 cell line after knocking down *Nup54* (Fig. S4B).

Discussion

SR proteins are a series of highly conserved serine/arginine-rich RNA binding proteins and are important splicing factors [24, 25]. SRSF1 is a member of the SR protein family [13]. *Srsf1* deletion in different tissues can lead to a variety of diseases, and *Srsf1* KO results in embryonic lethality in mice [21]. However, the role of SRSF1 in granulosa cell function is poorly understood. Our study showed that SRSF1 was expressed in both oocytes and granulosa cells during follicular development. To explore the role of SRSF1 in granulosa cells, we successfully knocked out SRSF1 in the granulosa cells of the primary follicles by *Foxl2-CreER^{T2}* mice. Morphological analysis of the ovaries showed that follicles of PfGC-*Srsf^{−/−}* ovaries were stunted, primary follicles failed to convert to secondary follicles, and a large number of atretic follicles were observed at 21 dpp. This study demonstrated that SRSF1 was required for follicle development in granulosa cells.

To further explore the cause of follicular atresia, we examined whether there were problems in the proliferation and apoptosis of granulosa cells. BrdU is an analogue of nucleotides and thymidine that is used to detect changes in proliferating cells [26]. BrdU staining of the ovary of 7dpp mice showed that the proliferation of PfGC-*Srsf1^{−/−}* granulosa cells was significantly slowed down. To further investigate the physiological status of reduced granulosa cell proliferation, TUNEL staining was performed on ovarian tissues at different developmental stages. The results showed that the number of apoptotic granulosa cells was increased in PfGC-*Srsf1^{−/−}*. This is consistent with previous reports, in which knockdown of *Srsf1* induces cell cycle arrest in mASMCs and inhibits mASMC proliferation [27], and SRSF1 regulates the apoptosis and proliferation and promotes the transformation of mammary epithelial cells [15]. These results indicate that SRSF1 regulates cell proliferation and apoptosis in different cell types.

To further investigate the effect of *Srsf1* deletion on granulosa cell development, 8 dpp ovaries were harvested for RNA-seq. The results showed that 881 genes were upregulated and 662 genes were downregulated at the transcriptome level. GO analysis of upregulated and downregulated genes revealed some associations with regulating the apoptotic signalling pathway, signal transduction by p53 class mediators, cell killing, and regulation of DNA repair-related signalling pathways. The results of qPCR verification were consistent with those of RNA-seq. These results suggest that SRSF1 may affect granulosa cell survival through multiple pathways.

SRSF1 may need to bind to a specific target pre-mRNA to perform its splicing function. We found that 249 genes underwent AS, and SEs accounted for the highest proportion. GO analysis was performed on the genes that were regulated by AS, and multiple phenotype-related signalling pathways were enriched. We successfully verified the AS of genes that are associated with signalling pathways such as DNA repair using RT−PCR. It has been documented that HERC2, NUP54, USP3, and CHD1L are involved in DNA repair in different cell types [28–35], and the present study showed that the expression of the DNA damage-related proteins USP3 and NUP54 was decreased in PfGC-*Srsf1^{−/−}*, which was closely related to POI [36, 37]. And knocking out *Nup54* in KK1 cell lines also causes DNA damage. Furthermore, the RIP results showed that SRSF1 directly binds to RNAs to regulate AS. However, SRSF1 regulates AS events related to the maintenance of survival and proliferation in dental progenitors by targeting *Cdc45*, *Incenp*, *Rif1*, *Ncor1*, *Cttn*, *Gak*, *Picalm*, *Hnrnpd*, *Srrm2*, and *Lsm6* pre-mRNAs [38]. Additionally, SRSF1 can regulate oocyte meiosis by binding to different target *Msh5* and *Six6os1* pre-mRNAs [19]. Thus, SRSF1 regulates the survival of different cells and development through AS.

In conclusion, our study showed that *Srsf1* deletion leads to abnormalities in multiple signalling pathways, such as DNA repair and cell killing. SRSF1 participation in AS affects DNA damage in granulosa cells, which in turn leads to follicular development arrest (Fig. 7). Abnormal AS can lead to granulosa cell apoptosis, which provides new information about clinical POI.

Availability of data and materials The authors confirm that the data supporting the findings of this study are available within the article and its supplementary materials. The RNA-seq data be deposited in GEO(https://www.ncbi.nlm.nih.gov/geo/query/acc.cgi?acc=GSE228975)under accession number GSE228975.

Declarations

Conflict of interest Conflict of interest statement. None declared.

Ethics approval and consent to participate This study was approved by China Agricultural University laboratory animal welfare and animal experimental ethical inspection (Issue No. AW11402202-3–6).

Consent for publication Not applicable.

References

1. Edson MA, Nagaraja AK, Matzuk MM (2009) The mammalian ovary from genesis to revelation. Endocr Rev 30(6):624–712. https://doi.org/10.1210/er.2009-0012
2. Li R, Albertini DF (2013) The road to maturation: somatic cell interaction and self-organization of the mammalian oocyte. Nat Rev Mol Cell Biol 14(3):141–152. https://doi.org/10.1038/nrm3531
3. Albertini DF (1992) Regulation of meiotic maturation in the mammalian oocyte: interplay between exogenous cues and the microtubule cytoskeleton. BioEssays 14(2):97–103. https://doi.org/10.1002/bies.950140205
4. Carabatsos MJ, Sellitto C, Goodenough DA, Albertini DF (2000) Oocyte-granulosa cell heterologous gap junctions are required for the coordination of nuclear and cytoplasmic meiotic competence. Dev Biol 226(2):167–179. https://doi.org/10.1006/dbio.2000.9863
5. Meduri G, Massin N, Guibourdenche J, Bachelot A, Fiori O, Kuttenn F, Misrahi M, Touraine P (2007) Serum anti-Mullerian hormone expression in women with premature ovarian failure. Hum Reprod 22(1):117–123. https://doi.org/10.1093/humrep/del346
6. Chon SJ, Umair Z, Yoon MS (2021) Premature ovarian insufficiency: past, present, and future. Front Cell Dev Biol 9:672890. https://doi.org/10.3389/fcell.2021.672890
7. Zhang QY, Li X, Zhou XY, Li Y, Zhang J, Zhang XF, Liu YD, Chen YX, Wu XM, Ma LZ, Chen X, Chen SL (2022) Study of differential proteomics in granulosa cells of premature ovarian insufficiency (POI) and the roles and mechanism of RAC1 in granulosa

8. Luan Y, Xu P, Yu SY, Kim SY (2021) The role of mutant p63 in female fertility. Int J Mol Sci. https://doi.org/10.3390/ijms22168968
9. Zhe J, Chen S, Chen X, Liu Y, Li Y, Zhou X, Zhang J (2019) A novel heterozygous splice-altering mutation in HFM1 may be a cause of premature ovarian insufficiency. J Ovarian Res 12(1):61. https://doi.org/10.1186/s13048-019-0537-x
10. Ghosh G, Adams JA (2011) Phosphorylation mechanism and structure of serine-arginine protein kinases. FEBS J 278(4):587–597. https://doi.org/10.1111/j.1742-4658.2010.07992.x
11. Cho S, Hoang A, Chakrabarti S, Huynh N, Huang DB, Ghosh G (2011) The SRSF1 linker induces semi-conservative ESE binding by cooperating with the RRMs. Nucleic Acids Res 39(21):9413–9421. https://doi.org/10.1093/nar/gkr663
12. Cho S, Hoang A, Sinha R, Zhong XY, Fu XD, Krainer AR, Ghosh G (2011) Interaction between the RNA binding domains of Ser-Arg splicing factor 1 and U1–70K snRNP protein determines early spliceosome assembly. Proc Natl Acad Sci U S A 108(20):8233–8238. https://doi.org/10.1073/pnas.1017700108
13. Das S, Krainer AR (2014) Emerging functions of SRSF1, splicing factor and oncoprotein, in RNA metabolism and cancer. Mol Cancer Res 12(9):1195–1204. https://doi.org/10.1158/1541-7786.MCR-14-0131
14. Anczukow O, Akerman M, Clery A, Wu J, Shen C, Shirole NH, Raimer A, Sun S, Jensen MA, Hua Y, Allain FH, Krainer AR (2015) SRSF1-regulated alternative splicing in breast cancer. Mol Cell 60(1):105–117. https://doi.org/10.1016/j.molcel.2015.09.005
15. Anczukow O, Rosenberg AZ, Akerman M, Das S, Zhan L, Karni R, Muthuswamy SK, Krainer AR (2012) The splicing factor SRSF1 regulates apoptosis and proliferation to promote mammary epithelial cell transformation. Nat Struct Mol Biol 19(2):220–228. https://doi.org/10.1038/nsmb.2207
16. Paz S, Ritchie A, Mauer C, Caputi M (2021) The RNA binding protein SRSF1 is a master switch of gene expression and regulation in the immune system. Cytokine Growth Factor Rev 57:19–26. https://doi.org/10.1016/j.cytogfr.2020.10.008
17. Katsuyama T, Moulton VR (2021) Splicing factor SRSF1 is indispensable for regulatory T cell homeostasis and function. Cell Rep 36(1):109339. https://doi.org/10.1016/j.celrep.2021.109339
18. Ye Y, Yu F, Li Z, Xie Y, Yu X (2021) RNA binding protein serine/arginine splicing factor 1 promotes the proliferation, migration and invasion of hepatocellular carcinoma by interacting with RecQ protein-like 4 mRNA. Bioengineered 12(1):6144–6154. https://doi.org/10.1080/21655979.2021.1972785
19. Sun L, Lv Z, Chen X, Wang C, Lv P, Yan L, Tian S, Xie X, Yao X, Liu J, Wang Z, Luo H, Cui S, Liu J (2023) SRSF1 regulates primordial follicle formation and number determination during meiotic prophase I. BMC Biol 21(1):49. https://doi.org/10.1186/s12915-023-01549-7
20. Wang H, Zhang Y, Zhang J, Du X, Li Q, Pan Z (2022) circSLC41A1 resists porcine granulosa cell apoptosis and follicular atresia by promoting SRSF1 through miR-9820–5p sponging. Int J Mol Sci. https://doi.org/10.3390/ijms23031509
21. Xu X, Yang D, Ding JH, Wang W, Chu PH, Dalton ND, Wang HY, Bermingham JR Jr, Ye Z, Liu F, Rosenfeld MG, Manley JL, Ross J Jr, Chen J, Xiao RP, Cheng H, Fu XD (2005) ASF/SF2-regulated CaMKIIdelta alternative splicing temporally reprograms excitation-contraction coupling in cardiac muscle. Cell 120(1):59–72. https://doi.org/10.1016/j.cell.2004.11.036
22. Zheng W, Zhang H, Gorre N, Risal S, Shen Y, Liu K (2014) Two classes of ovarian primordial follicles exhibit distinct developmental dynamics and physiological functions. Hum Mol Genet 23(4):920–928. https://doi.org/10.1093/hmg/ddt486

23. Hoage TR, Cameron IL (1976) Folliculogenesis in the ovary of the mature mouse: a radioautographic study. Anat Rec 184(4):699–709. https://doi.org/10.1002/ar.1091840409

24. Liu HX, Zhang M, Krainer AR (1998) Identification of functional exonic splicing enhancer motifs recognized by individual SR proteins. Genes Dev 12(13):1998–2012. https://doi.org/10.1101/gad.12.13.1998

25. Krainer AR, Conway GC, Kozak D (1990) The essential pre-mRNA splicing factor SF2 influences 5′ splice site selection by activating proximal sites. Cell 62(1):35–42. https://doi.org/10.1016/0092-8674(90)90237-9

26. Gratzner HG, Leif RC, Ingram DJ, Castro A (1975) The use of antibody specific for bromodeoxyuridine for the immunofluorescent determination of DNA replication in single cells and chromosomes. Exp Cell Res 95(1):88–94. https://doi.org/10.1016/0014-4827(75)90612-6

27. Guo YL, Chen ZC, Li N, Tian CJ, Cheng DJ, Tang XY, Zhang LX, Zhang XY (2022) SRSF1 promotes ASMC proliferation in asthma by competitively binding CCND2 with miRNA-135a. Pulm Pharmacol Ther 77:102173. https://doi.org/10.1016/j.pupt.2022.102173

28. Liu SS, Bai YS, Feng L, Dong WW, Li Y, Xu LP, Ma NF (2016) Identification of CHD1L as an important regulator for spermatogonial stem cell survival and self-renewal. Stem Cells Int. https://doi.org/10.1155/2016/4069543

29. Tsuda M, Cho K, Ooka M, Shimizu N, Watanabe R, Yasui A, Nakazawa Y, Ogi T, Harada H, Agama K, Nakamura J, Asada R, Fujiike H, Sakuma T, Yamamoto T, Murai J, Hiraoka M, Koike K, Pommier Y, Takeda S, Hirota K (2017) ALC1/CHD1L, a chromatin-remodeling enzyme, is required for efficient base excision repair. PLoS ONE 12(11):e0188320. https://doi.org/10.1371/journal.pone.0188320

30. Wang L, Chen K, Chen Z (2021) Structural basis of ALC1/CHD1L autoinhibition and the mechanism of activation by the nucleosome. Nat Commun 12(1):4057. https://doi.org/10.1038/s41467-021-24320-4

31. Bekker-Jensen S, Rendtlew Danielsen J, Fugger K, Gromova I, Nerstedt A, Lukas C, Bartek J, Lukas J, Mailand N (2010) HERC2 coordinates ubiquitin-dependent assembly of DNA repair factors on damaged chromosomes. Nat Cell Biol 12(1):80–86. https://doi.org/10.1038/ncb2008. (**sup pp 81-12**)

32. Izawa N, Wu W, Sato K, Nishikawa H, Kato A, Boku N, Itoh F, Ohta T (2011) HERC2 interacts with claspin and regulates DNA origin firing and replication fork progression. Cancer Res 71(17):5621–5625. https://doi.org/10.1158/0008-5472.CAN-11-0385

33. Rodriguez-Berriguete G, Granata G, Puliyadi R, Tiwana G, Prevo R, Wilson RS, Yu S, Buffa F, Humphrey TC, McKenna WG, Higgins GS (2018) Nucleoporin 54 contributes to homologous recombination repair and post-replicative DNA integrity. Nucleic Acids Res 46(15):7731–7746. https://doi.org/10.1093/nar/gky569

34. Lancini C, van den Berk PC, Vissers JH, Gargiulo G, Song JY, Hulsman D, Serresi M, Tanger E, Blom M, Vens C, van Lohuizen M, Jacobs H, Citterio E (2014) Tight regulation of ubiquitin-mediated DNA damage response by USP3 preserves the functional integrity of hematopoietic stem cells. J Exp Med 211(9):1759–1777. https://doi.org/10.1084/jem.20131436

35. Nicassio F, Corrado N, Vissers JH, Areces LB, Bergink S, Marteijn JA, Geverts B, Houtsmuller AB, Vermeulen W, Di Fiore PP, Citterio E (2007) Human USP3 is a chromatin modifier required for S phase progression and genome stability. Curr Biol 17(22):1972–1977. https://doi.org/10.1016/j.cub.2007.10.034

36. Takahashi A, Yousif A, Hong L, Chefetz I (2021) Premature ovarian insufficiency: pathogenesis and therapeutic potential of mesenchymal stem cell. J Mol Med (Berl) 99(5):637–650. https://doi.org/10.1007/s00109-021-02055-5

37. Wang X, Zhang X, Dang Y, Li D, Lu G, Chan WY, Leung PCK, Zhao S, Qin Y, Chen ZJ (2020) Long noncoding RNA HCP5 participates in premature ovarian insufficiency by transcriptionally regulating MSH5 and DNA damage repair via YB1. Nucleic Acids Res 48(8):4480–4491. https://doi.org/10.1093/nar/gkaa127

38. Yu T, Cazares O, Tang AD, Kim H-Y, Wald T, Verma A, Liu Q, Barcellos-Hoff MH, Floor SN, Jung H-S, Brooks AN, Klein OD (2022) SRSF1 governs progenitor-specific alternative splicing to maintain adult epithelial tissue homeostasis and renewal. Dev Cell 57(5):624-637.e624. https://doi.org/10.1016/j.devcel.2022.01.011